J Mater Sci (2010) 45:1560–1566
DOI 10.1007/s10853-009-4124-1

Mechanical properties of polycrystalline silicon solar cell feed stock grown via fluidized bed reactors

M. B. Zbib · M. C. Tarun · M. G. Norton · D. F. Bahr · R. Nair · N. X. Randall · E. W. Osborne

Received: 4 September 2009 / Accepted: 9 December 2009 / Published online: 29 December 2009

Abstract Polysilicon granular beads grown via a fluidized bed reactor, a feedstock for silicon solar cell production, were annealed, sectioned, and indented using a combination of nanoindentation and microhardness testing to determine the mechanical response of this commercially available raw material. The granular material, with macroscopic dimensions on the order of millimeters and an internal grain size on the order of 20 nm, has an indentation modulus of approximately 160 GPa, and a hardness prior to fracture of 9.6 GPa; these values are relatively insensitive to annealing at temperatures between 600 and 1100 °C. Indentation fracture testing suggests the toughness of this material is on the order of 0.6 MPa $m^{1/2}$. The fracture sequence has been verified using acoustic emission testing during indentation. Annealing in air at 600 °C for 3 days increases the toughness by approximately 50% with little change in grain size. The as grown material contains solute hydrogen, identified by infrared spectroscopy, from the growth process; annealing in air tends to remove solute hydrogen from the material at temperatures above 1050 °C. The removal of solute hydrogen appears to cause slight increases in toughness, while grain growth at elevated annealing temperatures or the formation of hydrogen complexes in the silicon appears to decrease toughness. The results suggest thermal treatments of silicon grown with this method can moderately alter the friability of the final product.

M. B. Zbib · M. C. Tarun · M. G. Norton · D. F. Bahr (✉)
Mechanical and Materials Engineering, Washington State University, Pullman, WA 99163, USA
e-mail: bahr@mme.wsu.edu

R. Nair · N. X. Randall
CSM Instruments Inc., Needham, MA 02494, USA

E. W. Osborne
REC Silicon, Moses Lake, WA 98837, USA

Introduction

High-purity polycrystalline silicon (polysilicon) is used for several purposes, including production of single crystal silicon, solar cell applications, and structures in micro-electro-mechanical systems (MEMS). For applications in which kilogram quantities of silicon are used at a time, most high-purity silicon is grown using chemical vapor deposition (CVD) from either trichlorosilane or silane gas in the Siemens process. Because of the high demand for photovoltaic materials, which now exceeds that used for producing silicon-integrated circuits, a relatively new method of polysilicon production has been developed; the fluidized bed reactor (FBR) [1]. The advantage of this method is in its lower cost than the traditional Siemens process, as it is more productive and less energy intensive. Existing FBR plants can generate up to 13,500 tons of polysilicon per year; as such it should be expected that FBR silicon will likely increase in usage and handling in the future.

The FBR method produces silicon as granules in a hydrogen-rich environment and results in a microstructure that has grain sizes in the 10s of nm regime [2]. Interspersed within FBR silicon are small pores, on the order of 5 μm, which are generally not present in polysilicon grown via other methods; growth in the Siemens process and standard MEMS processing usually provides a pore-free material. The inherent porosity suggests a possible propensity for fracture (i.e., flaw dominated strength behavior) in FBR material may be more of an issue than in material grown using other methods. In general, polysilicon from

the FBR process is produced using the thermal decomposition of trichlorosilane ($SiHCl_3$) or silane (SiH_4) via CVD in a bulk form that leads to the formation of 30–80-nm grains. The growth occurs at temperatures between 650 and 750 °C over approximately 1 day at these temperatures. Polysilicon grown using the Siemens' process has significantly larger grain sizes (on the order of 1–10 μm). Thin films of polysilicon, which have heavily twinned grains with sizes on the order of 1 μm are also produced using CVD at a range of temperatures, from 610 to >1040 °C [3]. Most MEMS processed polysilicon films also undergo post-growth heat treatments due to subsequent processing steps or to relieve residual stresses. Therefore, the structure of the FBR silicon may also lead to differences in properties from other, more studied, types of polysilicon.

Modern manufacturing centers of crystalline silicon solar cells (both single crystalline and polycrystalline) that rely upon melting feedstock polysilicon are generally remote from the production facilities for high-purity polysilicon. Producing polysilicon beads on commercial scales therefore requires the ability to move and ship these products, which will likely involve significant masses of beads in physical contact during transport. If fracture of the beads occurs it is possible that the friable materials will produce a fine silicon dust that makes subsequent handling particularly problematic from both practical and safety points of view. However, with silicon beads that have sizes on the order of 1–3 mm in diameter, conventional fracture testing is challenging. The intent of this study is to examine the mechanical properties of FBR silicon using indentation and indentation fracture testing with an aim toward determining if thermal processing during or after growth alters the toughness of the beads, and if the toughness of the FBR grown material is similar to that of other, more widely studied, systems.

The fracture behavior and testing of many forms of silicon has been extensively reviewed by Cook [4]. At room temperature, single crystal silicon is naturally brittle and there is no dislocation activity at the crack tip [5]. Numerous groups have made either toughness, strength, or fracture-resistance measurements using indentation or double cantilever beam techniques, resulting in reported fracture toughness, T, values that range from 0.6 to 0.95 MPa $m^{1/2}$. [6–12] In a manner similar to Cook, we choose to report T rather than a strictly mode-I fracture toughness, K_{Ic}, to account for the inherent ambiguity of the mode of fracture using indentation techniques. Cook [4] suggests that a reasonable toughness measured via indentation in (001) single crystals will range between 0.73 and 0.89 MPa $m^{1/2}$, with this as a metric it will be possible to rank changes in toughness with the particular morphology of FBR polycrystalline silicon and benchmark the testing method to that reported more widely in the literature.

The mechanical properties of bulk polysilicon and the effect of processing temperature tend to lead to slightly tougher materials than single crystal silicon. Earlier study in our group determined the fracture toughness of polysilicon grown via the Siemens process for as-grown and annealed materials with a grain size of approximately 3 μm [13]. For the as-grown material, T was 0.81 MPa $m^{1/2}$, and annealing altered the toughness of the material to between 0.57 and 1.11 MPa $m^{1/2}$. There was no clear trend in toughness with grain size in this material. Chen and Leipold [9] experimentally measured the toughness of polysilicon that includes precipitates and residual stress for large (2 mm) grains; this system had a fracture toughness of 0.75 MPa $m^{1/2}$. The fracture behavior of polycrystalline silicon grown by the Siemens' process using disk-shaped compact tension samples [14] showed toughness on the order of 1.5–1.8 MPa $m^{1/2}$ at room temperature; these values are noted in [4] to be sensitive to defects within macroscopic notches. Polysilicon films for MEMS, measured with a variety of methods ranging from micromachined samples to indentation-induced fracture, have toughness values between 0.9 and 1.9 MPa $m^{1/2}$ [3, 15–17]. There are two reasons for the wide range of reported properties for polysilicon. First, variations in deposition method and heat treatment conditions lead to differences in grain structure and residual stress. Secondly, many of the measurements using micromachined structures are not able to achieve a fine notch, which precludes use of the classical fracture mechanics approaches [4] and these tests are often dominated by flaw distribution.

In short, while it is reasonable to assume the toughness of polycrystalline silicon grown via FBR will be on the order of 1 MPa $m^{1/2}$, changes in thermal processing that previously have been shown to alter the toughness of bulk polycrystalline silicon by 50% could have a significant impact on the overall friability of the product. This study was carried out to determine the relative toughness of FBR grown polysilicon in both the as-grown condition as well as after the post-growth annealing treatments between 600 and 1100 °C.

Experimental

The specimens used for the experiment were supplied by REC Silicon (Moses Lake, WA). The specimens were in the form of beads that varied between 1 mm and 1 cm in diameter. Annealing was carried out in an open platinum crucible heated to 800 °C at 8 °C/min and then at a rate of 4 °C/min to the final annealing temperatures of 800–1100 °C. The annealed samples were held at the peak temperature for up to 6 h and then furnace cooled. After annealing, samples were mounted in an epoxy and then

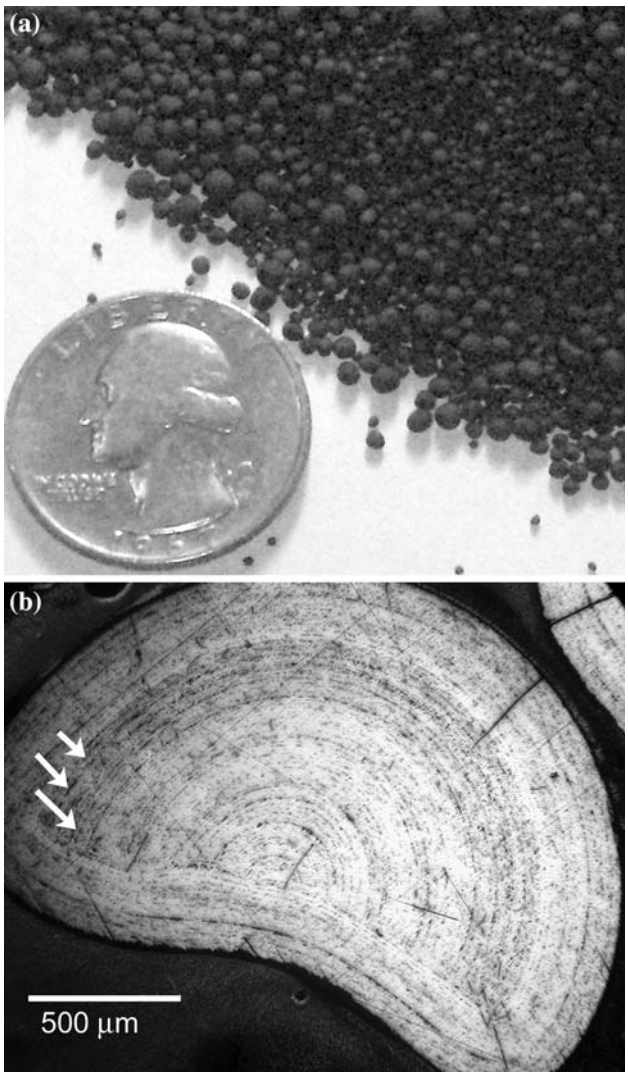

Fig. 1 **a** As-received FBR silicon morphology and **b** optical micrograph of the resulting microstructure of a bead that fractured during growth, showing distinctive regions of porosity in the sample noted with *arrows*

prepared by conventional methods of grinding and polishing as described in more detail by Dahl et al. [2]. The initial product and the microstructure of a granular bead that fractured during growth are shown in Fig. 1.

The mechanical properties were measured using three testing systems. Microhardness and fracture properties were carried out in a HVS-1000B Vickers microhardness tester. This system was used to cause indentation-induced fracture at applied loads between 0.245 and 2.94 N. Loads versus the average crack size were plotted to compare the behavior of different samples. A Hysitron Triboscope was used in conjunction with a Park Autoprobe CP scanning probe microscope for measuring the hardness and the elastic modulus of the studied samples at sizes smaller than the average pore spacing to ensure properties measurements were not influenced by the pre-existing pores. A quasi-static test was done with maximum applied loads between 5000 and 8500 µN, and the modulus and hardness were extracted using the Oliver and Pharr technique [18]. A CSM Instruments Micro-Combi Tester with a diamond Vickers indenter was used to determine the cracking sequence in this material by monitoring the acoustic emission during indentation. The acoustic emission sensor is directly integrated onto the indenter and operates with a frequency of 150 kHz over a dynamic range of 65 dB with amplification up to 200,000 times. When needed, images of the cracks were collected using scanning electron microscopy (SEM) with an FEI Sirion operated at 20 keV.

To perform infrared spectroscopy, the FBR silicon was ground with a mortar and pestle and mixed with infrared-transparent potassium bromide (KBr) powder and pressed into thin pellets of $\sim$0.3-mm thick. Infrared absorbance spectra were obtained with a Bomem DA8 Fourier transform infrared (FTIR) spectrometer with a KBr beam splitter. A liquid-nitrogen-cooled mercury cadmium telluride detector with a spectral range of 400–5000 cm^{-1} wavenumbers was used. Measurements were taken at an instrumental resolution of 4 cm^{-1}.

Results and discussion

Typical load–depth curves of nanoindentations in samples are shown in Fig. 2. The measured hardness and reduced modulus of polycrystalline silicon grown using FBR is relatively independent of the post-processing conditions for the range of temperatures and times used in this study. The hardness is between 9.1 and 10.0 GPa, the elastic modulus determined from indentation is between 142 and 166 GPa. The elastic modulus is calculated using

$$\frac{1}{E_R} = \frac{1-\nu_i^2}{E_i} + \frac{1-\nu_s^2}{E_s}; \quad (1)$$

the relation between the elastic modulus of the sample E_S, the reduced modulus as inferred from the unloading slope [18], and the Poisson's ratio of polysilicon, ν_S is 0.27 and ν_i for diamond is 0.07, assuming the modulus of the diamond indenter tip E_i is 1249 GPa. These results, along with similar measurements on single crystal silicon and bulk polycrystalline silicon grown via the Siemen's process, are shown in Table 1. There may be a bias in the measured modulus, as on the (001) single crystal silicon the values measured in this study are lower than the conventionally reported value of 163 GPa; this could be due to either tip or frame compliance calibration during nanoindentation. However, as the values are within 10% of typically reported values these data should be considered reasonable for sample-to-sample comparisons within this study.

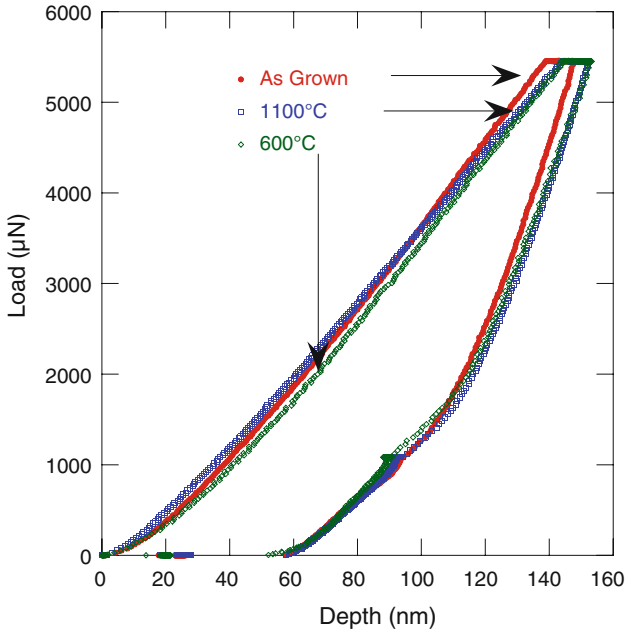

Fig. 2 A typical indentation load–depth curve of each as-grown, 1100 and 600 °C, samples showing no significant change in the hardness and reduced modulus values after different annealing conditions

The crack length as a function of applied load for each Vickers indentation was measured for each sample, with at least four measurements taken at each maximum load. A typical indentation-induced fracture is shown in Fig. 3 with crack lengths noted on the figure. The fracture toughness is related to the applied maximum load and the crack length by

$$T = \frac{\chi_r P}{c^{\frac{3}{2}}} \tag{2}$$

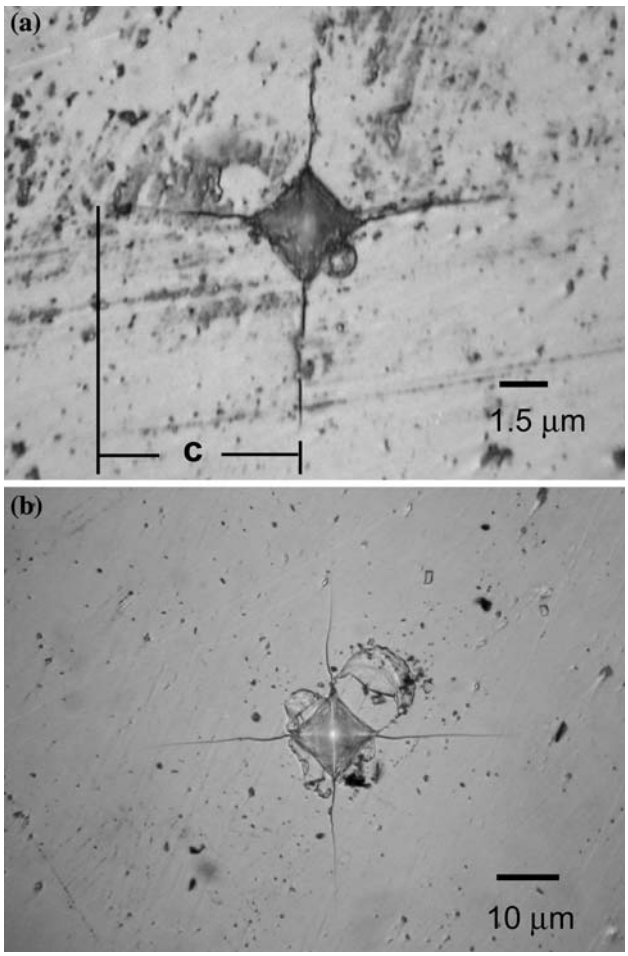

Fig. 3 **a** As-grown sample with an indentation of a 50-g load shows cracks that are not strongly influenced by the microstructure. **b** Annealed sample at 800 °C with an indentation load of 200 g, demonstrating that the presence of fine porosity does not influence the crack morphology

Table 1 Mechanical properties of granular silicon and reference materials as measured by nanoindentation and microhardness testing for fracture toughness

Sample	Hardness H (GPa)	Elastic modulus E (GPa)	$P/c^{3/2}$	Toughness (MPa $m^{1/2}$)	Grain size [2] (nm)
As-grown	9.7 ± 0.4	164 ± 3	9.1 ± 0.7	0.60 ± 0.05	30
600 °C (3 days)	9.6 ± 0.4	154 ± 7	14.5 ± 1.1	0.93 ± 0.08	45
600 °C (6 h)			11.3 ± 1.4	0.72 ± 0.09	
800 °C	9.1 ± 0. 7	159 ± 7	9.0 ± 1.2	0.60 ± 0.08	22
900 °C	9.5 ± 0.4	142 ± 3	6.6 ± 0.8	0.41 ± 0.05	38
1050 °C	9.4 ± 0. 6	166 ± 3	6.7 ± 0.9	0.45 ± 0.06	60
1100 °C	9.9 ± 0.8	149 ± 3	11.1 ± 2.0	0.69 ± 0.13	63
(001) Single crystal	9. 7 ± 0.3	146 ± 2	9.5 ± 2.0	0.61 ± 0.13	
Bulk polysilicon grown via Siemens process	10.0 ± 0.7	157 ± 3	11.5 ± 1.6	0.73 ± 0.10	>1000
Bulk annealed at 900 °C	9.7 ± 0.7	153 ± 3	15.1 ± 6.0	0.96 ± 0.38	>1000

The mean and standard deviation of between 16 and 28 tests for each sample is included in the table

where c is the average crack size, P is the applied indentation load, and χ_r is a constant dependant on the specific indenter-material system,

$$\chi_r = \xi\sqrt{\frac{E}{H}} \tag{3}$$

where H is the measured hardness of the material (measure with no cracking in this case to eliminate convolution of the properties), E is the measured elastic modulus, and ξ is the indenter invariant constant. For experiments with a Vickers tip in materials that do not undergo post-indentation or environmentally assisted crack growth after the indentation process is complete the indenter variant constant is 0.016 [19]. For each sample, the constant dependant of the specific material indenter-material system χ_r was calculated using Eq. 2 and then used in a least squares curve fit of Eq. 2 to verify toughness; these data and the resulting curve fits are shown in Fig. 4 along with the expected slope from the model in Eq. 2. In the case of the sample annealed at 600 °C for 6 h, the modulus and hardness ratio were assumed to be the same as that of the sample that was annealed at that temperature for 3 days.

The toughness for each of the systems is shown in Table 1. Standard deviations of between 16 and 28 tests for each sample are shown in the table, and the propagation of uncertainty based on these standard deviations and using the functional relationship of Eq. 2 was used to determine the standard deviation of the resulting toughness measurement. For clarity, Fig. 4 only shows the average values, and the fits to the toughness assuming a 2/3 power relationship are slightly different than the values presented in Table 1 due to differing numbers of tests performed at each load and the scatter present in the crack geometry measurements at the lowest loads in the bulk samples. Therefore, the actual toughness values determined are most accurately reflected in the tables (along with the uncertainty), and Fig. 4 is provided to demonstrate the extent of variation from the expected model.

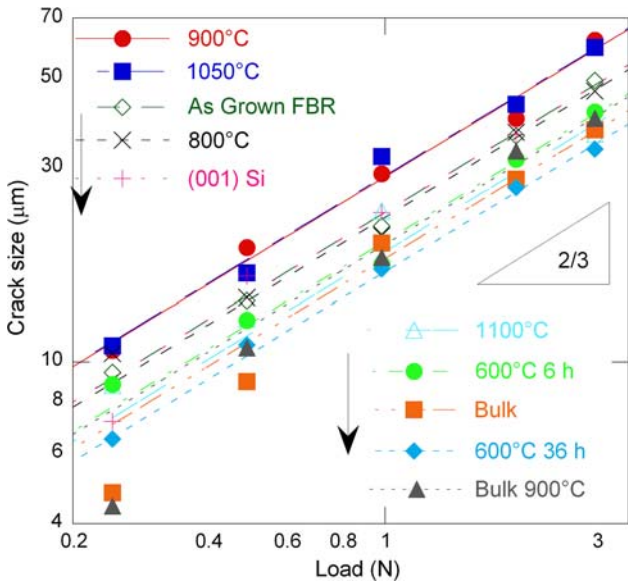

Fig. 4 Average crack radius versus load curves for various forms of silicon at different heat treatment conditions with the resulting curve fits for fracture toughness using Eq. 2

To verify the validity of the testing apparatus in these materials and ensure that the variation between these tests and the toughness model was minimal and not due to a differing fracture mode or morphology, a similar test was carried out in single crystal silicon and in bulk polycrystalline silicon. The value of toughness for (001) single crystal silicon is slightly outside the range noted by Cook [4] for indentation-induced toughness measurements in that orientation of silicon (about 0.1 MPa $m^{1/2}$ lower), however, these crack length tests and measurements were not specifically aligned with any particular direction, which may add to the lower than expected toughness values. The toughness for annealed bulk polycrystalline silicon was approximately 0.7 MPa $m^{1/2}$, also approximately 0.1 MPa $m^{1/2}$ lower than reported in our earlier study, but similar to values found previously [13]. These two control tests suggest that the toughness inferred from indentation is reasonable and comparable to other published studies, and is likely providing a lower bound estimate of the toughness of the FBR silicon. In particular, the consistency of this study suggests that the current methodology for measurements is appropriate for providing relative comparisons between samples that have undergone various processing conditions.

To use the mechanics for indentation fracture testing, the sequence of fracture should follow that for which the methods were developed. Fused silica is a common material used in the development of these tests; in silica the fracture sequence begins during loading and continues during unloading [20, 21]. Since indentation in these samples cannot be used in conjunction with optical microscopy to verify the fracture sequence, indentation fracture was monitored using acoustic emission during a series of indentations, shown in Fig. 5. Fracture in the FBR polysilicon follows a sequence similar to that in silica since it starts during loading, as shown in Fig. 5, with increased acoustic emission activity that we assume is related to fracture events. Also, as noted in Fig. 3, the existence of porous regions of material did not impact the fracture geometry of the indentation fracture, suggesting the toughness measurements are representative of the material as a whole and not influenced by the pre-existing flaws.

FBR polysilicon, which uses a significant amount of H_2 as a carrier gas, does have the potential to incur trapped H within the solid. To identify the presence of either dissolved or surface-bound H, FTIR was carried out on both

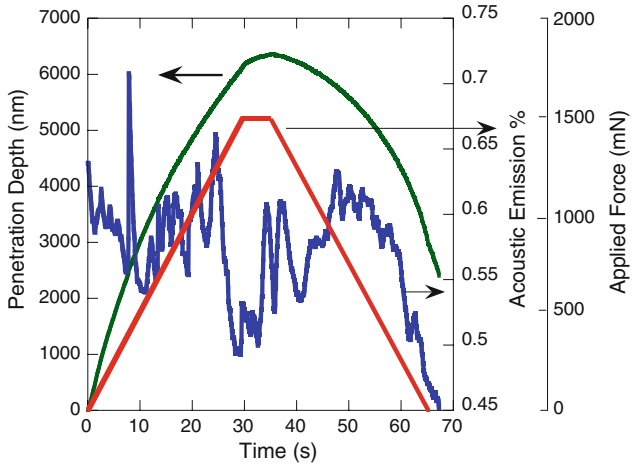

Fig. 5 Acoustic emission curve demonstrates that cracking is occurring during both loading and unloading, which verifies the use of the indentation fracture toughness models

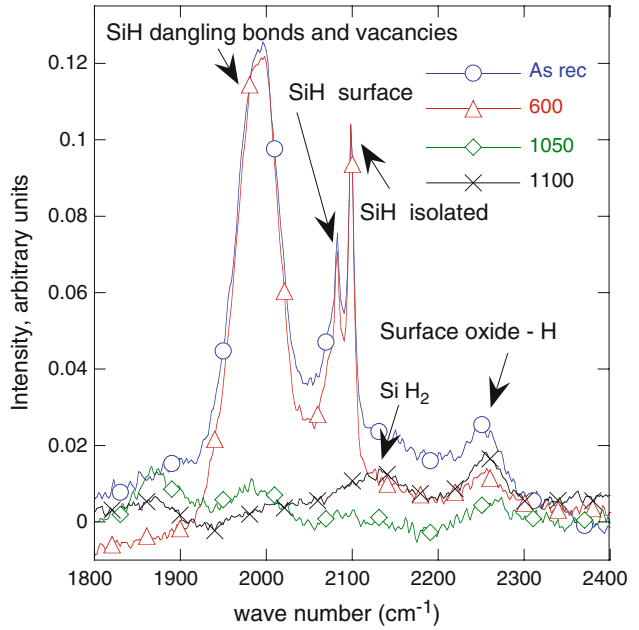

Fig. 6 Normalized FTIR spectra of as grown and annealed FBR polysilicon; background subtracted to highlight Si–H peaks. The amount of H dissolved in the samples decreases with increasing annealing temperature. Peak identification based on [22]

as-grown and annealed granular material. The FTIR spectra, with the background subtracted, is shown in Fig. 6 for wavenumbers between 2400 and 1900 cm^{-1}. The peaks at 2081 and 2097 can be ascribed to Si–H bonds on the surface; there are literature reports of peaks present at 2083 being linked to Si–H coupled to other clusters on the surface, while 2090 has been identified as isolated Si–H bonds [22]. After annealing, the samples were ground with a mortar and pestle; therefore, the surface area of the samples is dominated by internal porosity, rather than the external free surface. It would therefore be expected that H bonded to the surface of the sample may be based on H present in the pores, and subsequent annealing would involve transport to these internal free surfaces. The broad peak around 1985 has been attributed to internal Si–H bonds linked to dangling bonds and vacancies within the solid, while peaks near 2110 are likely due to Si–H_2 bonds and the peak near 2280 is related to Si–O–H bonds present on free surfaces (which could easily have formed during annealing in the ambient air atmosphere). While these data are not quantitatively analyzed in this study, the amount of H present within the lattice clearly decreases at higher annealing temperatures. This change in composition may well be responsible for changes in toughness with different annealing conditions.

Conclusions

Polycrystalline silicon grown in a FBR, with grain sizes on the order of 20–60 nm, has a fracture toughness that is about 20% lower than polysilicon grown via the Siemens process, but a similar elastic modulus and hardness to the bulk polysilicon material. Annealing FBR polysilicon in air at moderate temperatures (600 °C) to remove solute hydrogen increases the toughness to values that correspond to that of material grown using the Siemens process, approximately 1 MPa $m^{1/2}$; the change in toughness is likely due to the elimination of solute hydrogen, rather than changes in grain size. The presence of micron scale porosity in the FBR material does not dramatically alter the crack morphology generated by indentation testing. Subsequent annealing processes at higher temperatures lead to degradation in the toughness, which may be related to associated changes in microstructure or the formation of defects within the solid from solute H that does not desorb during annealing. The friability of polysilicon grown with the FBR technique can be altered slightly by post-growth thermal treatments, but to first order can be treated as a material with similar properties as conventionally processed bulk polysilicon.

Acknowledgements We would like to thank M.M. Dahl for help in sample preparation, microscopy for Fig. 1, and technique development in the handling of silicon granules grown by the FBR.

References

1. Caussat B, Hemati M, Couderc JP (1995) Chem Eng Sci 50:3615
2. Dahl MM, Bellou A, Bahr DF, Norton MG, Osborne EW (2009) J Cryst Growth 311:1496
3. Ballarini R, Mullen RL, Yin Y, Kahn H, Stemmer S, Heuer AH (1997) J Mater Res 12:915

4. Cook RF (2006) J Mater Sci 41:841. doi:10.1007/s10853-006-6567-y
5. Chiao YH, Clarke DR (1989) Acta Met 37:203
6. John CFSt (1975) Philos Mag 32:1193
7. Brede M, Hansen P (1988) Acta Met 36:2003
8. Hirsch PB, Samuels J, Roberts SG (1989) Proc R Soc Lond A 421:25
9. Chen CP, Leipold MH (1980) Am Ceram Soc Bull 59:469
10. George A, Michot G (1993) Mater Sci Eng A 164:118
11. Ericson F, Johansson S, Schweitz JA (1988) Mat Sci Eng A 105:131
12. Ebrahimi F, Kalwani L (1999) Mat Sci Eng A 268:116
13. Fancher RW, Watkins CM, Norton MG, Bahr DF, Osborne EW (2001) J Mater Sci 36:5441. doi:10.1023/A:1012425529753
14. Brodie RC, Bahr DF (2003) Mat Sci Eng A 351:166
15. Sharpe WN, Yuan B, Edwards RL (1997) Mat Res Soc Symp Proc 505:51
16. Tsuchiya T, Sakata J, Taga Y (1997) Mat Res Soc Symp Proc 505:285
17. Kahn H, Tayebi N, Ballarini R, Mullen RL, Heuer AH (2000) Sens Actuators A 82:274
18. Oliver WC, Pharr GM (1992) J Mater Res 7:1564
19. Morris DJ, Cook RF (2005) Int J Fract 136:237
20. Morris DJ, Vodnick AM, Cook RF (2005) Int J Fract 136:265
21. Cook RF, Pharr GM (1990) J Am Ceram Soc 73:787
22. von Keudell A, Abelson JR (1998) J Appl Phys 84:489